





Restoring Images in Adverse Weather Conditions via Histogram Transformer

Shangquan Sun^{1,2} , Wenqi Ren^{3,4†} , Xinwei Gao⁵, Rui Wang^{1,2} , and
Xiaochun Cao³ 

¹ Institute of Information Engineering, Chinese Academy of Sciences, Beijing 100085, China

² School of Cyber Security, University of Chinese Academy of Sciences, Beijing 100049, China

³ School of Cyber Science and Technology, Shenzhen Campus of Sun Yat-sen University, Shenzhen 518107, China

⁴ Guangdong Provincial Key Laboratory of Information Security Technology, Guangzhou 510006, China

⁵ Wechat Business Group, Tencent, Shenzhen, Guangdong, China, 518057
shangquansun@gmail.com, renwq3@mail.sysu.edu.cn,

Overview

In the supplementary material, we first present additional quantitative results, notably the results of non-reference image quality assessments in Section 1, an experiment of user studies in Section 2, and the comparison of model complexities in Section 3. Furthermore, we show more visual comparisons among the existing adverse weather removal methods in Section 4 including paired and unpaired test data.

1 Non-reference Image Quality Assessment on Real-world Unpaired Data

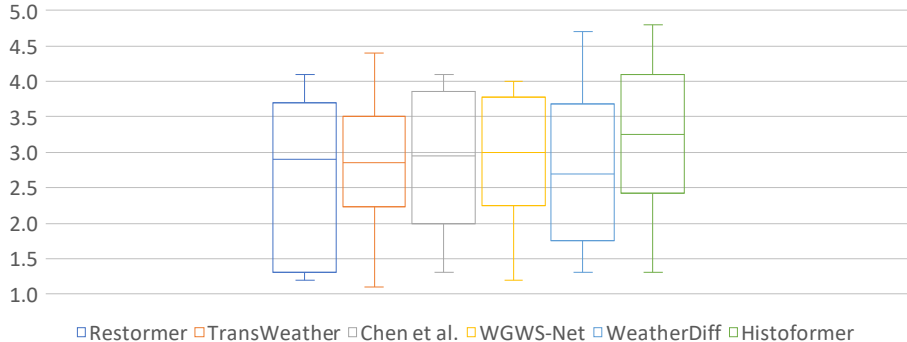
Due to the absence of ground-truths for real rainy images in the real-world test set of Snow100K [4], we conduct the qualitative comparison through the computation of non-reference image quality assessment metrics, specifically NIQE [6] and BRISQUE [5], applied to a randomly selected subset of 20 images. The results are illustrated in Table 1. Evidently, our approach attains superior image quality based on both non-reference metrics. Additional visual examples will be presented in the subsequent Section 4.

2 User Study

In this section, we conduct a user study using a subset of 20 images randomly selected from the real-world degraded test set of Snow100K [4]. Six methods

Table 1: The metrics comparison of real-world adverse weather removal for non-reference image quality assessment on Snow100K [4].

	Input	TransWeather [10]	Chen <i>et al.</i> [1]	WGWS-Net [15]	WeatherDiff ₆₄ [7]	WeatherDiff ₁₂₈ [7]	Ours
NIQE↓		2.68	3.58	3.47	3.51	3.30	3.32 1.80
BRISQUE↓		18.37	19.64	20.98	21.23	20.67	20.73 13.53

**Fig. 1:** The boxplot of the mean opinion score for each method.

are selected for comparison, namely Restormer [12], TransWeather [10], Chen *et al.* [1], WGWS-Net [15], WeatherDiff₆₄ and our Histoformer for comparison. The evaluation employs Mean Opinion Score, ranging from 1 (indicating poor visual quality) to 5 (representing excellent quality), for each sample. Ten participants, spanning ages 12 to 70, contribute to a total of 1,200 data of scores. For each input degraded image, we align it with the results restored by the aforementioned six methods in a group. Method names are concealed from participants, and the six images are shuffled to ensure a fair comparison. Users are instructed to assess the restoration quality relative to the input degraded image. After score collection, mean scores for each image are computed by averaging across participants. Subsequently, boxplot for each method are drawn and depicted in Figure 1. Notably, all methods yield mean opinion scores around 3.0, indicating a “fair” quality compared to the degraded inputs. However, our method achieves the optimal overall performance in terms of median, the third quartile and maximum scores, in line with the visual comparison detailed in the subsequent Section 4.

3 Performance and Complexities

We further compare our method with the recent adverse weather removal models, considering both model size and computational complexities. Additionally, we present the adverse weather removal results in terms of PSNR and SSIM on Outdoor-Rain [2] for convenient reference to their restoration performances. The

Table 2: The performances of deweathering, space and computational complexities of the existing deweathering methods. The PSNR and SSIM are tested on Outdoor-Rain [2] and the results of FLOPs are computed on the inputs of 256×256 .

	All-in-One [3]	TransWeather [10]	Chen <i>et al.</i> [1]	WGWS-Net [15]	WeatherDiff ₆₄ [7]	WeatherDiff ₁₂₈ [7]	Ours
PNSR	24.71	28.83	28.47	28.65	29.64	29.72	32.08
SSIM	0.8980	0.9000	0.9107	0.9207	0.9312	0.9216	0.9389
#Param	44.00M	38.05M	28.71M	5.19M	82.92M	85.56M	16.61M
FLOPs	12.26G	12.24G	49.22G	13.61G	475.16G	263.45G	91.59G

values are detailed in Table 2. Evidently, our method exhibits comparable model size and computation overhead as the previous methods, although it does not surpass some among them. It is noteworthy that both the feed-forward and the histogram self-attention are computed in dual-branches, and their complexities could be condensed by the technique of model pruning. Addressing the matter of model efficiency will be pursued leveraging techniques in model compression, such as pruning and quantization. Overall, our method attains a reasonable balance between the restoration quality and model complexities.

4 More Visual Comparisons

In this section, we present additional samples for visual comparison on weather-degraded datasets, including Figure 2 and 3 from Snow100K-L [4], Figure 4 and 5 from Outdoor-Rain [2], Figure 6 and 7 from RainDrop [8], and Figure 8 and 14 from Snow100K [4].

The first two test sets possess synthetic degradation, while the latter two comprise real-world data for two tasks of rain drop removal and desnowing respectively. For the task of real-world deraining and dehazing, we evaluate the weather removal methods on real rainy images from Internet-Data [11] and present visual comparison results in Figure 15 and 16. Notably, RainDrop [8] is a real-world dataset containing ground-truths.

As depicted, our Histoformer consistently demonstrates results closely aligning with the ground-truths on paired data and exhibits superior visual quality on unpaired data.



Fig. 2: A visual comparisons of desnowing on Snow100K-L [4].



Fig. 3: A visual comparisons of desnowing on Snow100K-L [4].

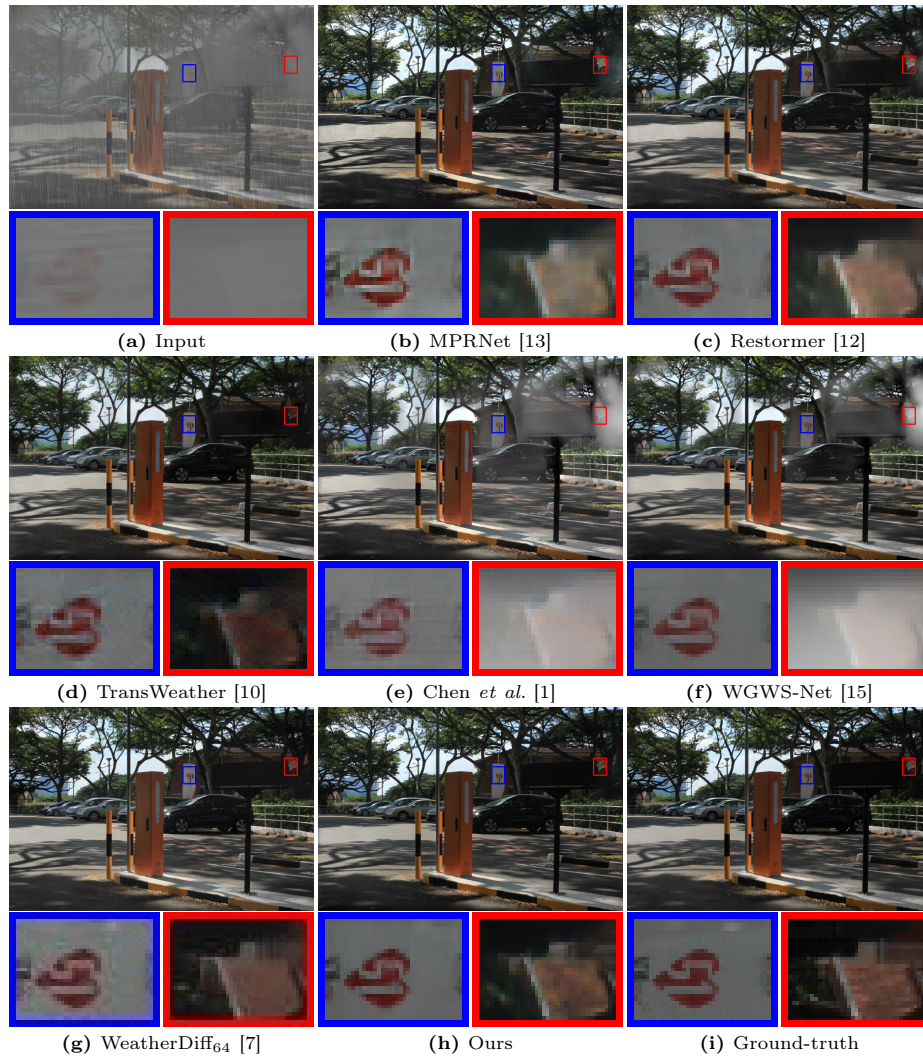


Fig. 4: A visual comparison of rain streak and haze removal on Outdoor-Rain [2].

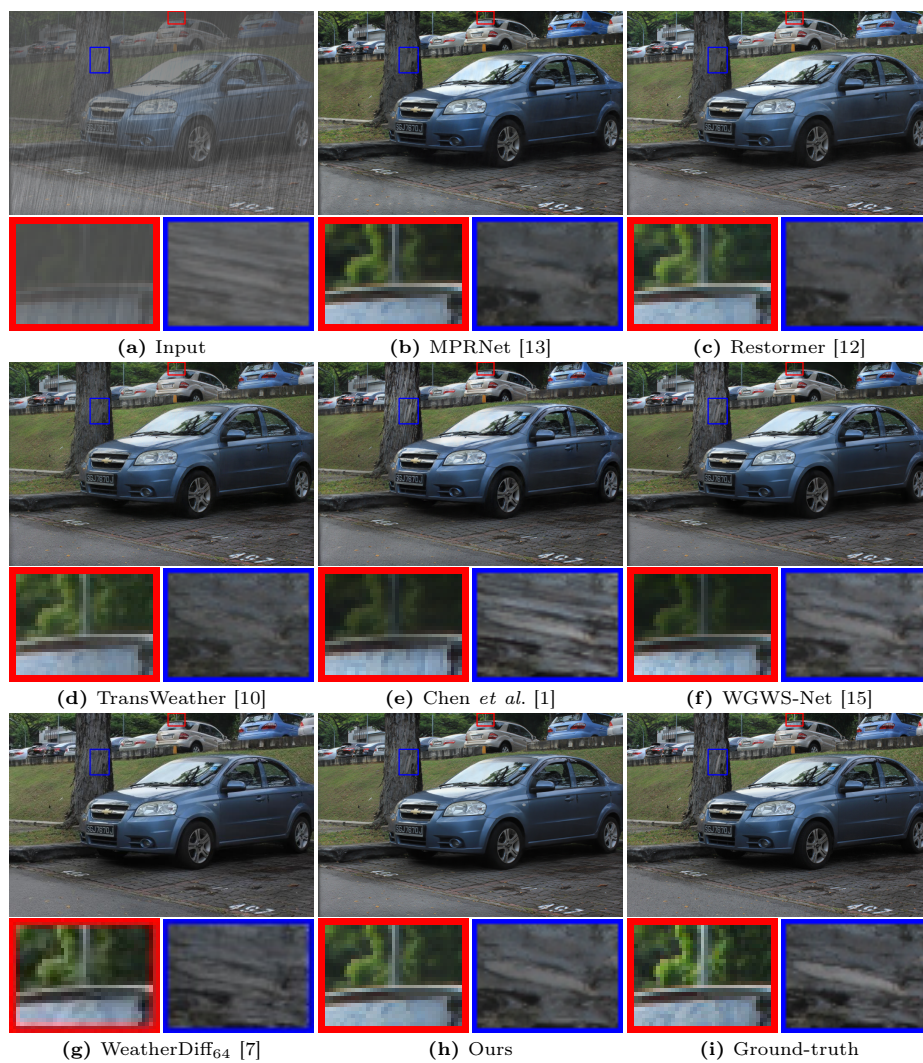


Fig. 5: A visual comparison of rain streak and haze removal on Outdoor-Rain [2].



Fig. 6: A visual comparison of real-world raindrop removal on RainDrop [8].

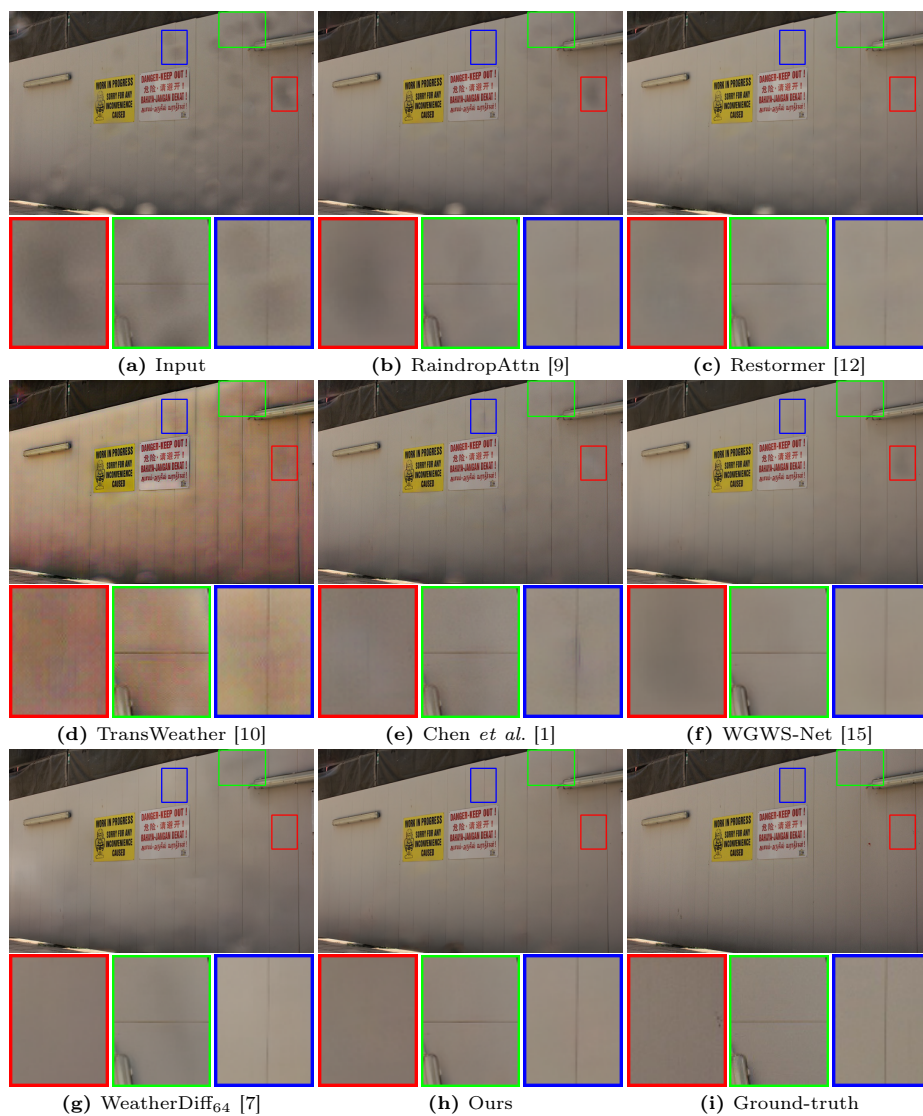


Fig. 7: A visual comparison of real-world raindrop removal on RainDrop [8].

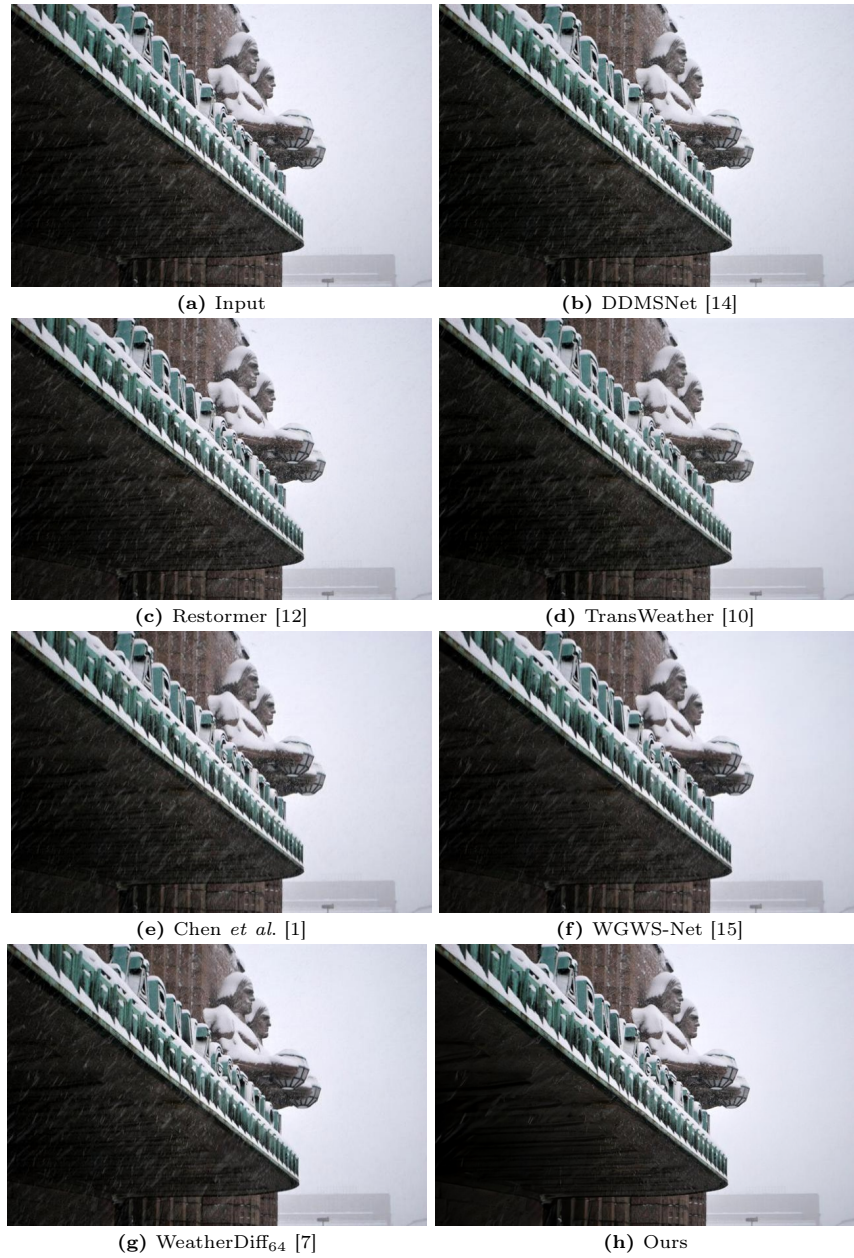


Fig. 8: A visual comparison of real-world desnowing on Snow100K [4].



Fig. 9: A visual comparison of real-world desnowing on Snow100K [4].

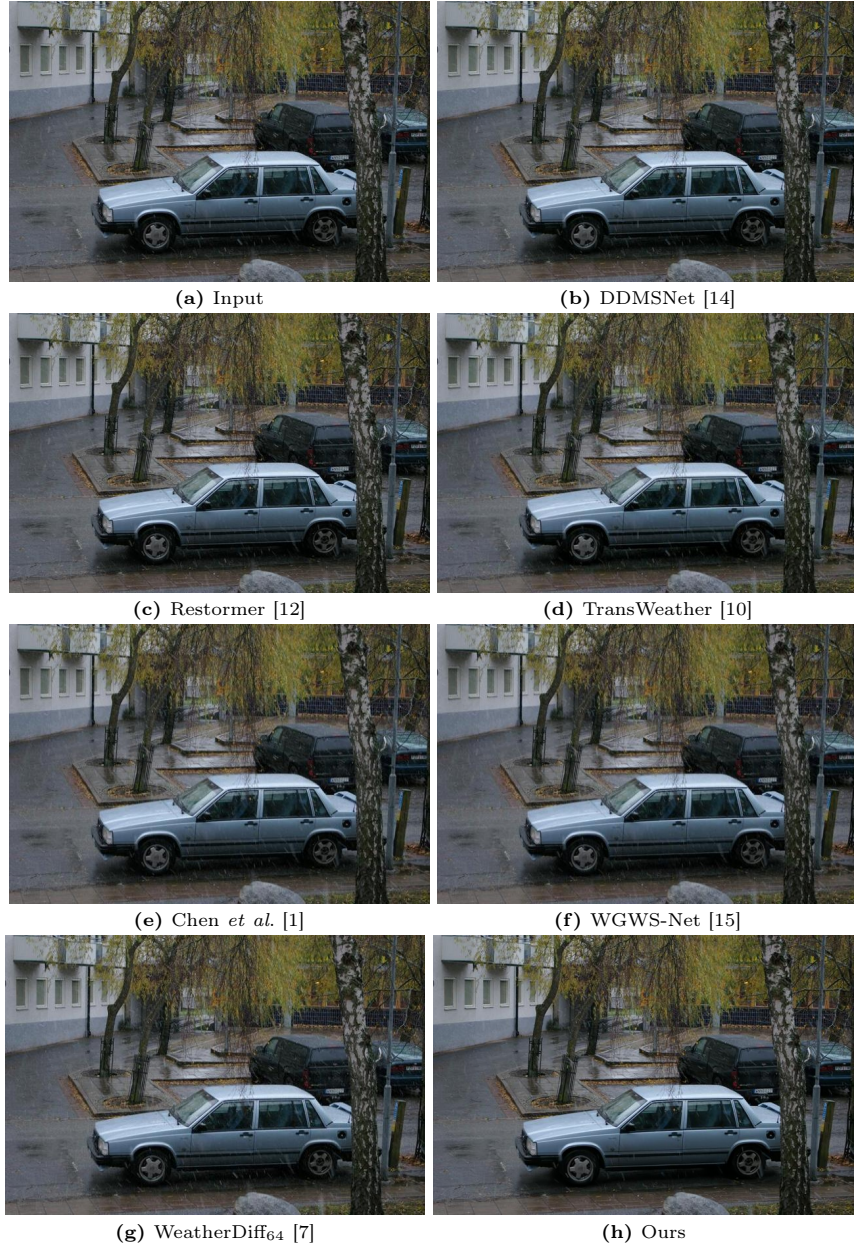


Fig. 10: A visual comparison of real-world desnowing on Snow100K [4].

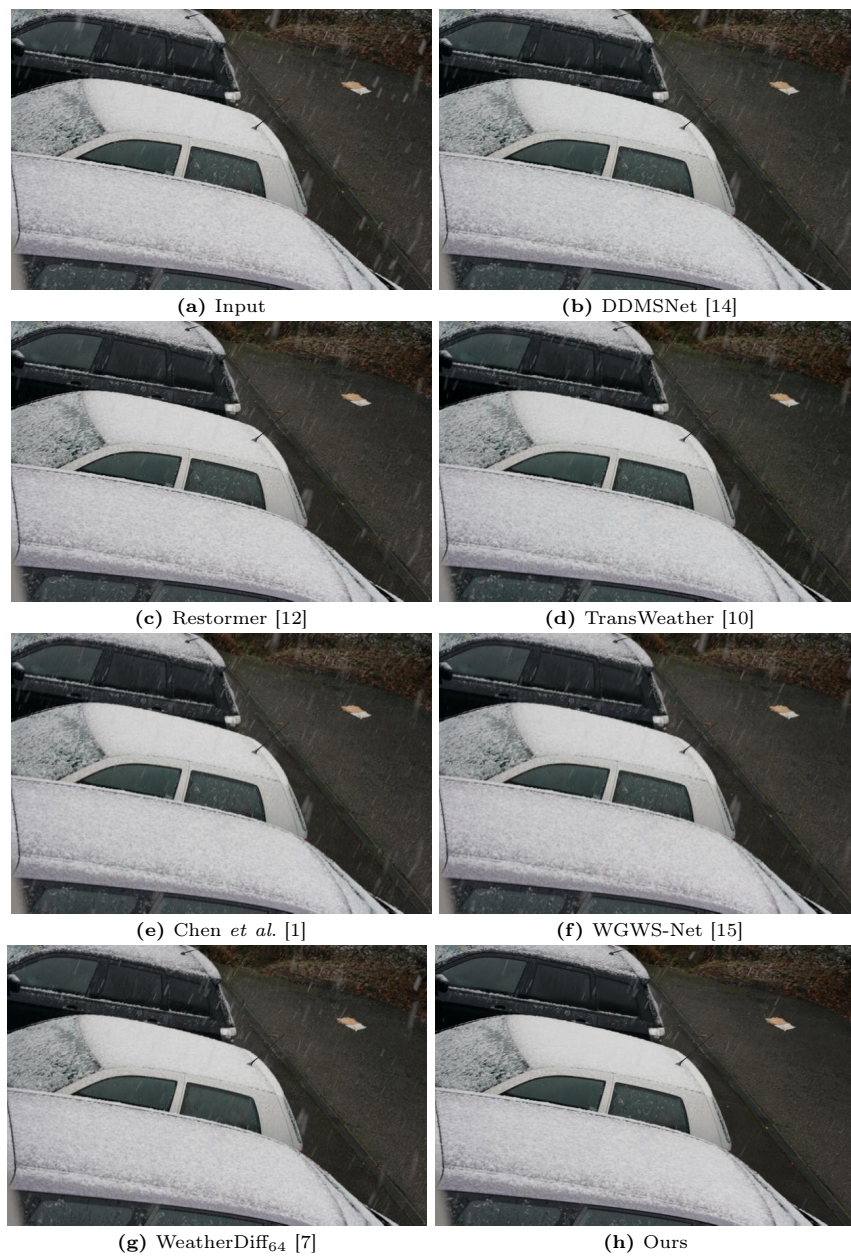


Fig. 11: A visual comparison of real-world desnowing on Snow100K [4].

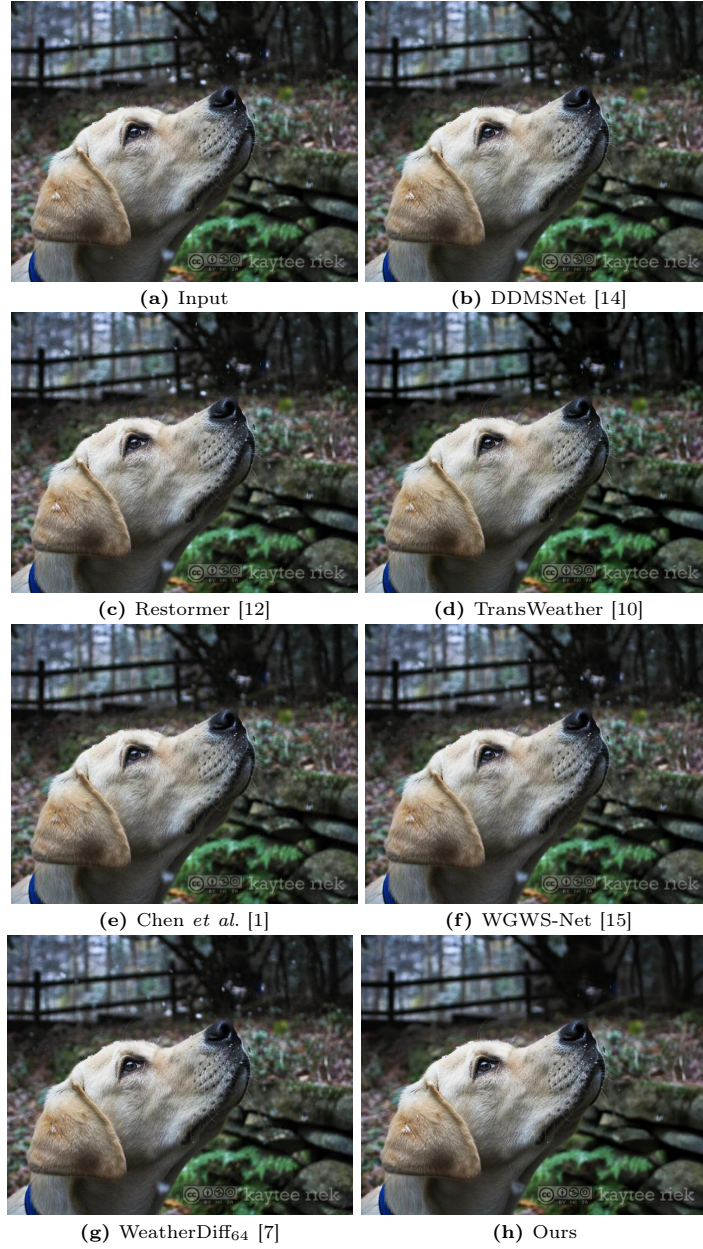


Fig. 12: A visual comparison of real-world desnowing on Snow100K [4].



Fig. 13: A visual comparison of real-world desnowing on Snow100K [4].

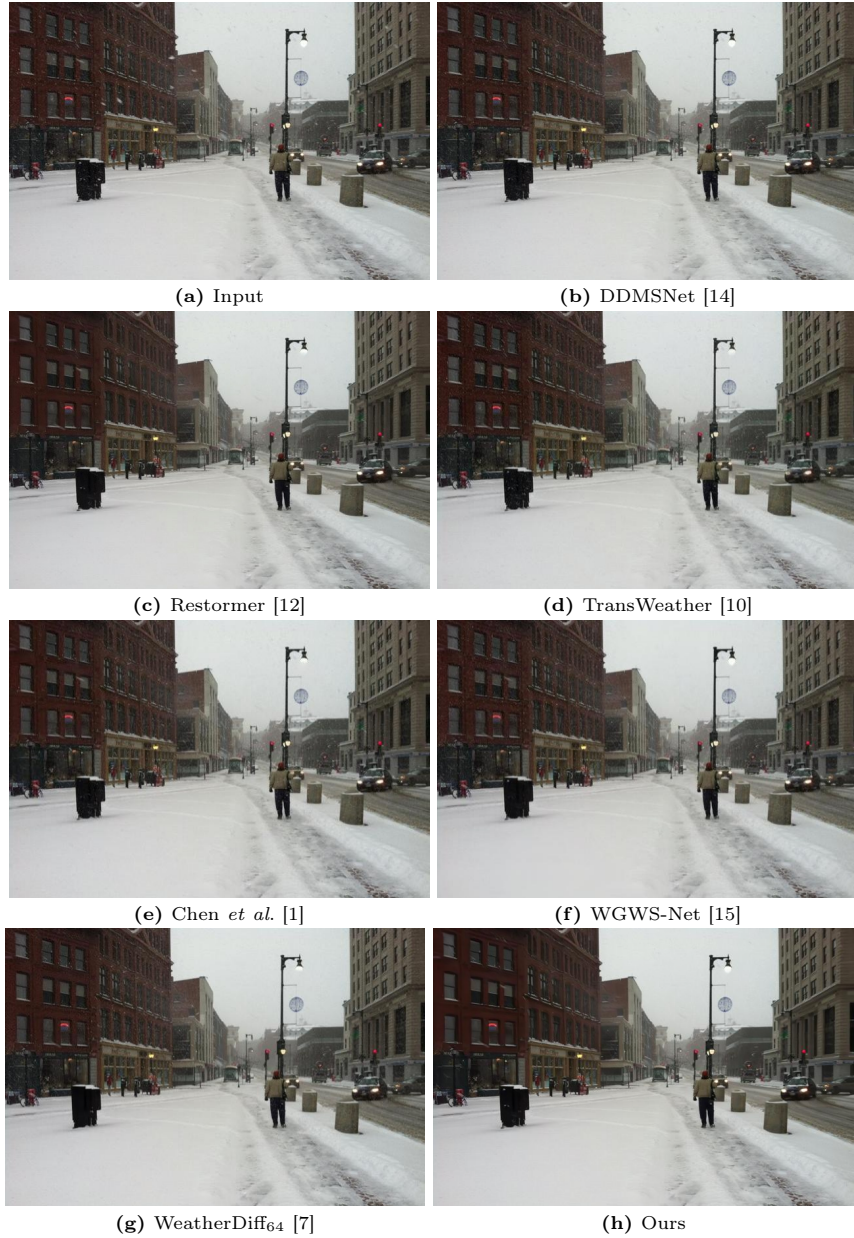


Fig. 14: A visual comparison of real-world desnowing on Snow100K [4].



Fig. 15: A visual comparison of real-world rain streak and haze removal from Internet-Data [11].

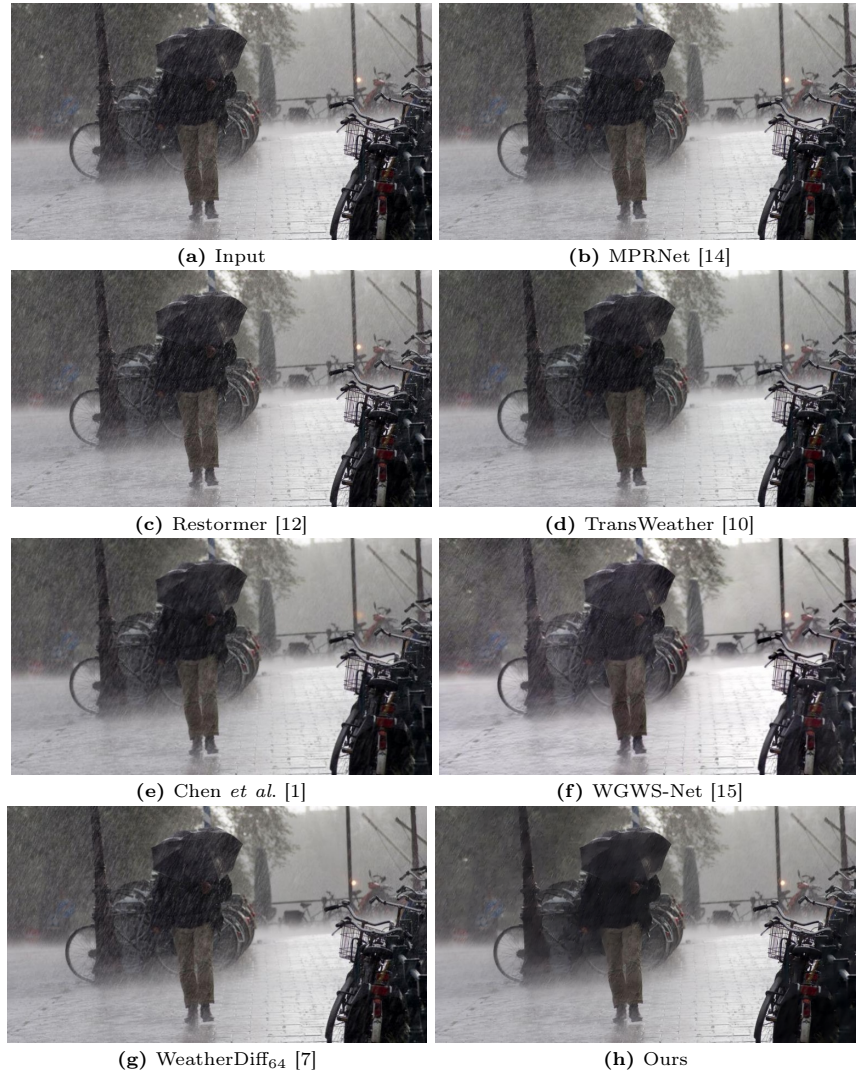


Fig. 16: A visual comparison of real-world rain streak and haze removal from Internet-Data [11].

References

1. Chen, W.T., Huang, Z.K., Tsai, C.C., Yang, H.H., Ding, J.J., Kuo, S.Y.: Learning multiple adverse weather removal via two-stage knowledge learning and multi-contrastive regularization: Toward a unified model. In: CVPR (2022)
2. Li, R., Cheong, L.F., Tan, R.T.: Heavy rain image restoration: Integrating physics model and conditional adversarial learning. In: CVPR (2019)
3. Li, R., Tan, R.T., Cheong, L.F.: All in one bad weather removal using architectural search. In: CVPR (2020)
4. Liu, Y.F., Jaw, D.W., Huang, S.C., Hwang, J.N.: Desnownet: Context-aware deep network for snow removal. IEEE TIP (2018)
5. Mittal, A., Moorthy, A.K., Bovik, A.C.: No-reference image quality assessment in the spatial domain. IEEE TIP (2012)
6. Mittal, A., Soundararajan, R., Bovik, A.C.: Making a “completely blind” image quality analyzer. IEEE Signal processing letters (2012)
7. Özdenizci, O., Legenstein, R.: Restoring vision in adverse weather conditions with patch-based denoising diffusion models. IEEE TPAMI (2023)
8. Qian, R., Tan, R.T., Yang, W., Su, J., Liu, J.: Attentive generative adversarial network for raindrop removal from a single image. In: CVPR (2018)
9. Quan, Y., Deng, S., Chen, Y., Ji, H.: Deep learning for seeing through window with raindrops. In: ICCV (2019)
10. Valanarasu, J.M.J., Yasarla, R., Patel, V.M.: Transweather: Transformer-based restoration of images degraded by adverse weather conditions. In: CVPR (2022)
11. Wang, T., Yang, X., Xu, K., Chen, S., Zhang, Q., Lau, R.W.: Spatial attentive single-image deraining with a high quality real rain dataset. In: CVPR (2019)
12. Zamir, S.W., Arora, A., Khan, S., Hayat, M., Khan, F.S., Yang, M.H.: Restormer: Efficient transformer for high-resolution image restoration. In: CVPR (2022)
13. Zamir, S.W., Arora, A., Khan, S., Hayat, M., Khan, F.S., Yang, M.H., Shao, L.: Multi-stage progressive image restoration. In: CVPR (2021)
14. Zhang, K., Li, R., Yu, Y., Luo, W., Li, C.: Deep dense multi-scale network for snow removal using semantic and depth priors. IEEE TIP (2021)
15. Zhu, Y., Wang, T., Fu, X., Yang, X., Guo, X., Dai, J., Qiao, Y., Hu, X.: Learning weather-general and weather-specific features for image restoration under multiple adverse weather conditions. In: CVPR (2023)